Astronomy & Astrophysics manuscript no. MeCN˙6
March 21, 2019

Rotational spectra of isotopic species of methyl cyanide, CH_3CN, in their ground vibrational states up to terahertz frequencies

Holger S. P. Müller[1], Brian J. Drouin[2], and John C. Pearson[2]

[1] I. Physikalisches Institut, Universität zu Köln, Zülpicher Str. 77, 50937 Köln, Germany
e-mail: hspm@ph1.uni-koeln.de
[2] Jet Propulsion Laboratory, California Institute of Technology, Mail Stop 183-301, 4800 Oak Grove Drive, Pasadena, CA 91011-8099, USA

Received 21 July 2009 / Accepted 18 August 2009

ABSTRACT

Context. Methyl cyanide is an important trace molecule in star-forming regions. It is one of the more common molecules used to derive kinetic temperatures in such sources.
Aims. As preparatory work for Herschel, SOFIA, and in particular ALMA we want to improve the rest frequencies of the main as well as minor isotopologs of methyl cyanide.
Methods. The laboratory rotational spectrum of methyl cyanide in natural isotopic composition has been recorded up to 1.63 THz.
Results. Transitions with good signal-to-noise ratio could be identified for CH_3CN, $^{13}CH_3CN$, $CH_3^{13}CN$, $CH_3C^{15}N$, CH_2DCN, and $^{13}CH_3^{13}CN$ in their ground vibrational states up to about 1.2 THz. The main isotopic species could be identified even in the highest frequency spectral recordings around 1.6 THz. The highest J'' quantum numbers included in the fit are 64 for $^{13}CH_3^{13}CN$ and 89 for the main isotopic species. Greatly improved spectroscopic parameters have been obtained by fitting the present data together with previously reported transition frequencies.
Conclusions. The present data will be helpful to identify isotopologs of methyl cyanide in the higher frequency bands of instruments such as the recently launched Herschel satellite, the upcoming airplane mission SOFIA or the radio telescope array ALMA.

Key words. molecular data – methods: laboratory – techniques: spectroscopic – radio lines: ISM – ISM: molecules

1. Introduction

Methyl cyanide, CH_3CN, also known as acetonitrile, or cyanomethane, was among the early molecules to be detected by radio astronomical means. Solomon et al. (1971) detected it almost 40 years ago toward the massive star-forming regions Sagittarius A and B close to the Galactic center. It has been detected in dark clouds such as TMC-1 (Matthews & Sears 1983), around the low-mass protostar IRAS 16293−2422 (Cazaux et al. 2003), in the circumstellar shell of the famous carbon-rich star IRC +10216 (Agúndez et al. 2008), in comets, such as Kohoutek (Ulich & Conklin 1974), and in external galaxies (Mauersberger et al. 1991). As a strongly prolate symmetric top, meaning $A \gg B$, transitions with different K but the same J occur in fairly narrow frequency regions, but sample rather different energies. Therefore, CH_3CN is quite commonly used to derive the kinetic temperatures of dense molecular clouds as already done in Solomon et al. (1971) or in e. g. Cummins et al. (1983). In less dense clouds the large dipole moment of 3.922 D (Gadhi et al. 1979) may prevent thermal equilibration. In that case, the isoelectronic methyl acetylene, or propyne, CH_3CCH, is often used instead.

The $^{12}C/^{13}C$ ratio in the vicinity of the Galactic center is approximately 20 (Wilson & Rood 1994; Müller et al. 2008). Thus, it is not surprising that the two isotopomers containing ^{13}C were detected fairly soon after the detection of the main isotopolog. $CH_3^{13}CN$ (Cummins et al. 1983) was detected first probably by accident because the isotopic substitution at the central C-atom does not change the spectroscopic parameters much with respect to the main species. Sutton et al. (1985) detected lines of both isotopomers with one ^{13}C in a line survey of Orion. More recently, CH_2DCN has been detected in two hot core sources (Gerin et al. 1992), and some lines of $CH_3C^{15}N$ were detected in a line survey of Sagittarius B2 (Nummelin et al. 1998).

A plethora of high-resolution spectroscopic investigations have been performed on methyl cyanide. It was actually among the first molecules to be studied by microwave spectroscopy by Ring et al. (1947). Cazzoli & Puzzarini (2006) reviewed the investigations for the main isotopic species and performed high resolution, high accuracy measurements up to 1.2 THz. Pearson & Müller (1996) analogously presented data up to 607 GHz for the singly substituted ^{13}C isotopomers as well as for the species with ^{15}N. Le Guennec et al. (1992) built on the very small data set for CH_2DCN by measuring an isotopically enriched sample up to 471 GHz. Finally, there has been only one report on the isotopolog with two ^{13}C which was restricted to frequencies up to 72 GHz (Tam et al. 1988).

We have measured rotational spectra of methyl cyanide in natural isotopic composition both in wide frequency windows as well as selected lines up to 1.63 THz to provide new or updated catalog entries for various isotopologs of methyl cyanide as well as for excited vibrational states. With rotational temperatures of CH_3CN in hot cores reaching at least 150−200 K (Sutton et al. 1985; Belloche et al. 2009), these data will be of great relevance for the Atacama Large Millimeter Array (ALMA). The main isotopolog and possibly even the ^{13}C isotopomers or the $v_8 = 1$ excited vibrational state will be seen with the HIFI instrument (Heterodyne Instrument for the Far-Infrared) on board of the recently launched Herschel satellite or with SOFIA (Stratospheric

Observatory For Infrared Astronomy). In the present article we provide the ground state rotational data obtained for six different isotopic species: CH_3CN, $^{13}CH_3CN$, $CH_3^{13}CN$, $CH_3C^{15}N$, CH_2DCN, and $^{13}CH_3^{13}CN$; as usual, unlabeled atoms refer to ^{12}C and ^{14}N. Analyses of selected excited vibrational states are currently under way.

2. Experimental details

Individual transitions have been recorded with the Cologne Terahertz Spectrometer (CTS) which has been described in detail by Winnewisser et al. (1994). It uses broadband tunable, phase-locked backward-wave oscillators (BWOs) as powerful sources, and a magnetically tuned, liquid helium cooled hot-electron InSb bolometer as detector. In the present case, one BWO was used to record transitions between 249 and 340 GHz.

The pressure of methyl cyanide in the 3 m long absorption cell was around 0.3−0.5 Pa. The measurements were carried out in static mode, and the sample was pumped off and replaced about every half hour.

The accuracies with which lines can be measured with the CTS depend on the lines shape, mostly on how symmetric the line is, and on the signal-to-noise (S/N) ratio. Quite commonly, we reach relative accuracies of 10^{-8} or even slightly better (Müller & Brünken 2005; Müller et al. 2007a, 2008). Müller et al. (2000) have shown that similar accuracies can be achieved for the rare isotopolog $SO^{17}O$ in a rather dense spectrum. The lines recorded for $^{13}CH_3CN$, $CH_3^{13}CN$, and $CH_3C^{15}N$ had very good S/N ratios and line shapes. Thus, the uncertainties were judged to be ≤ 10 kHz. The lines of CH_2DCN and $^{13}CH_3^{13}CN$ were considerably weaker such that uncertainties of up to 30 kHz were assigned.

The majority of the data has been extracted from broad frequency scans taken with the JPL cascaded multiplier spectrometer (Drouin et al. 2005). Generally, a multiplier chain source is passed through a 1 − 2 meter pathlength flow cell and is detected by a silicon bolometer cooled to near 1.7 K. The cell is filled with a steady flow of reagent grade acetonitrile and the pressure and modulation are optimized to enable good S/N ratios with narrow lineshapes. With a gas with very strong transitions, such as the $K < 7$ transitions of the main isotopolog of acetonitrile, the S/N ratio was optimized for a higher-K transition (e.g. $K = 12$) such that the lower K transitions exhibit saturated line profiles. This procedure enables better dynamic range for the extraction of line positions for rare isotopologs and highly excited vibrational satellites. The frequency ranges covered were 440−540, 619−631, 638−648, 770−855, 875−930, 967−1050, 1083−1093, 1100−1159, 1168−1198, 1576−1591, and 1614−1627 GHz. Most of these multiplier sources were previously described (Drouin et al. 2005). However, the multiplier chain with frequency range coverage between 967−1050 GHz was not described in that work. This chain consists of two cascaded triplers after the amplified W-band stage, the peak output power is near 100 μW. The efficiency of frequency multipliers usually changes strongly with frequency. In addition, recording conditions and sensitivities of detectors can have strong influences on the quality of the spectra. Particularly good S/N ratios were reached around 630, 900 and around 1100−1200 GHz. The spectra around 500 and around 800 GHz had poorer S/N ratios. In addition, the S/N ratios changed considerably within each scan and were usually lower towards the ends. Uncertainties of 50 kHz were assigned to isolated lines with good to very good S/N ratios throughout the frequency regions. Larger uncertainties were assigned to weaker lines or lines which were not isolated. In the course of the analysis it was observed that several strong lines had residuals considerably smaller than 50 kHz. Thus, smaller uncertainties, down to 20 kHz, were assigned to very strong lines, depending on the symmetry of the line shape.

Table 1. Lower state quantum numbers of rotational transitions[a] of CH_3CN from present work, frequencies (MHz), uncertainties unc. (kHz), and residuals o−c (kHz) between observed frequencies and those calculated from the final set of spectroscopic parameters.

J''	K''	frequency	unc.	o−c
86	15	1584230.365	150	−155
86	14	1585042.686	100	39
86	13	1585800.110	100	4
86	12	1586502.584	50	−32
86	11	1587149.953	50	35
86	10	1587741.807	50	39
86	9	1588277.964	50	22
86	8	1588758.221	50	−15
86	7	1589182.509	50	44
86	6	1589550.454	50	−11
86	5	1589862.092	50	−2
86	4	1590117.262	50	32
86	3	1590315.822	50	50
86	2	1590457.643	50	−1
86	1	1590542.824	50	34
86	0	1590571.147	50	−28
87	9	1606303.437	100	75
87	8	1606788.347	50	71
87	7	1607216.562	50	−25
87	6	1607588.178	50	50
87	5	1607902.790	50	35
87	4	1608160.351	50	6
87	3	1608360.834	50	36
87	2	1608504.060	50	25
87	1	1608590.002	50	3
87	0	1608618.661	50	3
88	10	1623774.391	50	9
88	9	1624320.812	50	−33
88	8	1624810.328	50	−27
88	7	1625242.737	50	13
88	6	1625617.728	50	−56
88	5	1625935.334	50	−57
88	4	1626195.369	50	−52
88	3	1626397.725	50	−47
88	2	1626542.355	50	−11
88	1	1626629.131	50	−14
88	0	1626658.067	50	−7

[a] Transitions are $J''+1, K'' \leftarrow J'', K''$ for all isotopologs except for CH_2DCN.

3. Analysis and discussion

The previously available data set will be described in the following for each isotopolog individually, with the exception of the two singly substituted ^{13}C species because the latter had almost always been investigated together. The extent of lines added in the course of the present work will be given also.

The main isotopolog of methyl cyanide as well as all other ones investigated in the present work are strongly prolate symmetric rotors having C_{3v} symmetry, except for CH_2DCN. Spin-statistics have to be taken into account for the symmetric rotor isotopologs. Levels having $K = 3n \pm 1$ belong to the E symmetry

class whereas levels having $K = 3n$ belong to the A symmetry class; $n \geq 0$ in all instances. The spin-statistical weight of A symmetry levels with $K > 0$ is twice that of $K = 0$ and all E symmetry levels.

The observed transitions all obey the $\Delta K = 0$ selection rule thus their positions are unaffected by the purely K-dependent parameters. However, these parameters are not negligible as they affect the intensities of the $\Delta K = 0$ transitions due to their contribution to the energies of the rotational levels.

In a strongly prolate molecule, such as methyl cyanide, $\Delta K = 3$ transitions only gain intensity through centrifugal distortion effects; they were too weak to be identified unambigously in the present work. Because of this, the purely K-dependent parameters A, D_K, etc. are usually not determinable for such molecules by means of rotational spectroscopy.

The dipole moment has been measured both for CH_3CN (Gadhi et al. 1979) and $CH_3C^{15}N$ (Mito et al. 1984). Isotopic differences in the dipole moments are expected to be small for the symmetric top species. In the case of $CH_3C^{15}N$, a value was obtained that deviated barely significantly (3.9256 (7) D) from the value for the main isotopolog (3.92197 (13) D).

CH_2DCN is the only asymmetric top rotor among the isotopologs dealt with in the present article. It only has C_S symmetry, therefore, no spin-statistics have to be considered, in contrast to what was assumed in Gerin et al. (1992). The asymmetry parameter $\kappa = (2B-A-C)/(A-C)$ is -0.9973, expectedly close to the prolate symmetric top limit of -1. The small rotation of the inertial axis system caused by the substitution of one H atom by D gives rise to a small b-dipole moment component of ~0.17 D. ΔK_a and ΔK_c have to be odd for b-type transitions. However, most of the previously observed and all of the new transitions are a-type transitions with $\Delta K_a = 0$ and $\Delta K_c = 1$. Transitions having $\Delta K_a = 2$ are allowed also, but are very weak for asymmetric molecules close to the prolate symmetric limit.

3.1. CH_3CN

Cazzoli & Puzzarini (2006) carried out extensive high resolution, high accuracy measurements on CH_3CN up to 1.2 THz. Their data set also included data from Kukolich et al. (1973); Kukolich (1982); Boucher et al. (1977) below 74 GHz. Šimečková et al. (2004) pointed to an interaction between $v = 0$, $K = 14$ and the lowest excited, doubly degenerate $v_8 = 1$ bending mode at $K = 12$ in the lower energy $l = +1$ component causing non-negligible shifts between $J'' \approx 36$ and 48. However, they were only able to perform a preliminary analysis because they only observed $J'' = 38$ and 39 of $v = 0$. A more complete analysis has been presented by Müller et al. (2007b); a manuscript on this work, involving extensive rotational and rovibrational data for states with $v_8 \leq 2$, is in preparation. The perturbation is negligible for all but the small number of $v = 0$, $K = 14$ transitions. Thus, in the present analysis, the perturbed transitions were omitted from the final fit. No evidence for perturbations was found in the rotational spectra of the less abundant isotopologs.

37 lines have been detected around 1.6 THz covering $J'' = 86$ to 88 with K up to 15. These data are given in Table 1 together with their assignments, uncertainties, and the residuals between measured frequencies and those calculated from the final spectroscopic parameters. They have been fit together with previous data mentioned above which extended to $K = 21$ and $J'' = 64$. Also included in the fits were the $\Delta K = 3$ ground state energy differences from Anttila et al. (1993) in order to determine the purely K-dependent terms A and D_K. Tunable far-infrared data from Pavone et al. (1990) were omitted from the final fits because trial fits with these data included showed their effect on the spectroscopic parameters to be negligible.

The considerable extension of the data set in J required two additional higher order parameters to be included in the fit, the decic centrifugal distortion parameters P_{JK} and P_{JJK}, as shown in Table 2. On the other hand, the centrifugal distortion correction term eQq_J has been omitted from the final fit because it was not significantly determined, (31 ± 15) Hz, and because it may still be too large in magnitude even though the absolute value in Cazzoli & Puzzarini (2006) was more than one order of magnitude smaller than that in Šimečková et al. (2004). If one assumes the ratio of $-D_J/B$ to be a good estimate for the ratio of eQq_J/eQq then the eQq_J value in Cazzoli & Puzzarini (2006) is about one order of magnitude too large, but has presumably the correct (positive) sign; Šimečková et al. (2004) determined a negative value. As the hyperfine parameters and the lower order distortion terms are mostly determined by the data published by Cazzoli & Puzzarini (2006) it is not surprising that there is a good agreement between the parameter values and uncertainties determined both in that study as well as in the present work. The increase in J in the present study causes the purely J-dependent terms (B, ..., L_J) to be improved in accuracy despite the additional centrifugal distortion terms.

The purely K-dependent terms A and D_K are determined in the present study entirely by the $\Delta K = 3$ ground state energy differences from Anttila et al. (1993). Thus, good agreement is not surprising. Trial fits with H_K released yielded a value of (155 ± 102) Hz as in Anttila et al. (1993). Judging by the D_K/A ratio, it is too large by about a factor of 3. Moreover, the parameter has not been determined with significance. Therefore, H_K was fixed in the present analysis to a value derived from the D_K/A ratio. Current results from the more extended analysis (Müller et al. 2007b) are in support of this value.

The weighted standard deviation of the fit is 0.906, indicating that the data have been reproduced within experimental uncertainties on average. The corresponding value for only the new transition frequencies is 0.670, suggesting the estimates of the uncertainties to be slightly too conservative.

3.2. $^{13}CH_3CN$ and $CH_3^{13}CN$

The data set of Pearson & Müller (1996) contained besides their new measurements of the rotational spectra for the two singly substituted ^{13}C isotopomers data from Demaison et al. (1979) for both species, covering 71−184 GHz as well as data for the $J = 2 - 1$ transitions for $CH_3^{13}CN$ from Kukolich (1982).

The terrestrial $^{12}C/^{13}C$ ratio is about 90. Hence, transitions of these species were easily observable in samples of natural isotopic composition, see Fig. 1. It is worthwhile mentioning that transitions of the main isotopolog in excited vibrational states $v_8 = 1$ and 2 and $v_4 = 1$ having the same K are about as strong or even stronger at room temperature than the transitions of the ^{13}C isotopomers.

262 and 244 transitions were used in the final fits of $^{13}CH_3CN$ and $CH_3^{13}CN$ from the broad spectral recordings. J'' was extended to 66 and 64, respectively, near 1.2 THz and K reached 16 and 15, respectively. Some transitions were even identified near 1.6 THz, but they were too few and of too poor S/N to have a signifant impact on the data sets. The weighted standard deviation for the lines measured at JPL are 0.854 and 0.875, respectively, indicating essentially appropriate error estimates on average.

Table 2. Spectroscopic parameters[a] (MHz) of methyl cyanide isotopic species with C_{3v} symmetry and dimensionless weighted standard deviation wrms.

Parameter	CH_3CN	$CH_3^{13}CN$	$^{13}CH_3CN$	$^{13}CH_3^{13}CN$	$CH_3C^{15}N$
$(A-B)\times10^{-3}$	148.900 074 (65)	148.904 624	149.165 664	149.171 692	149.176 934
B	9 198.899 134 (11)	9 194.349 983 (27)	8 933.309 412 (28)	8 927.281 294 (155)	8 922.038 611 (72)
D_K	2.825 1 (15)	2.825 7	2.825 7	2.825 7	2.825 7
$D_{JK}\times10^3$	177.407 96 (28)	176.673 95 (132)	168.239 65 (130)	167.420 4 (177)	168.938 0 (34)
$D_J\times10^3$	3.807 528 (9)	3.809 706 (37)	3.624 918 (32)	3.627 152 (61)	3.555 206 (45)
$H_K\times10^6$	51.	51.	51.	51.	51.
$H_{KJ}\times10^6$	6.063 1 (16)	6.001 9 (131)	5.803 1 (141)	5.50 (42)	5.641 0 (181)
$H_{JK}\times10^6$	1.025 61 (18)	1.017 52 (86)	0.927 05 (86)	0.915 9 (35)	0.950 83 (131)
$H_J\times10^{12}$	−255.96 (245)	−270.2 (61)	−283.0 (49)	−298.	−197.7 (67)
$L_{KKJ}\times10^{12}$	−446.3 (26)	−440.	−433.	−427.	−425.
$L_{JK}\times10^{12}$	−52.58 (64)	−49.40 (236)	−49.45 (266)	−47.3	−48.
$L_{JJK}\times10^{12}$	−7.889 (45)	−7.730 (141)	−6.843 (128)	−6.7	−7.041 (182)
$L_J\times10^{15}$	−1.80 (19)	−1.80	−1.80	−1.80	−1.28
$P_{JK}\times10^{18}$	529. (119)	530.	450.	450.	440.
$P_{JJK}\times10^{18}$	56.1 (29)	56.	48.	48.	49.
eQq	−4.223 24 (108)	−4.218 30 (176)	−4.218 13 (197)	−4.213 19	n. a.
$C_{bb}\times10^3$	1.785 (92)	1.785	1.73	1.73	–
$(C_{aa}-C_{bb})\times10^3$	−1.24 (31)	−1.24	−1.24	−1.24	–
wrms	0.906	0.813	0.760	0.635	0.692

[a] Numbers in parentheses are one standard deviation in units of the least significant figures. Parameters without quoted uncertainties have been estimated from the main isotopic species and were kept fixed in the fits; see section 3.

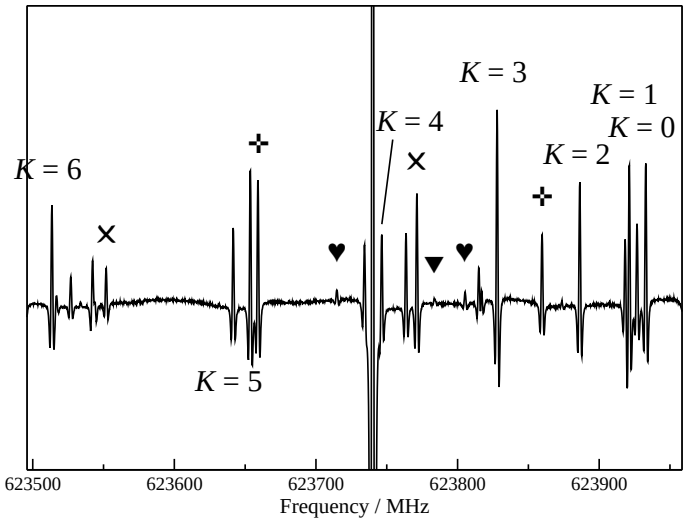

Fig. 1. Section of the submillimeter spectrum of CH_3CN. Transitions of $CH_3C^{15}N$ have been labeled with their K quantum numbers. $K = 3$ and 6 appear stronger than expected because of the spin-statistics, see section 3. Also labeled are $K = 10$ and 9 of $^{13}CH_3CN$ by x-signs, $K = 9$ and 8 of $CH_3^{13}CN$ by plus-signs, $K = 9$ of CH_2DCN by an inverted triangle, and $k = -15$ and +17 of CH_3CN, $v_8 = 1$ by heart-signs. The strong, clipped line in the center of the figure is due to $K = 10$ of CH_3CN, $v = 0$. The remaining unlabeled transitions have not been assigned thus far. $K = 10$ of CH_2DCN as well as three transitions of $^{13}CH_3^{13}CN$ are too weak to be recognized on this scale. The lines appear as second derivatives of a Gaussian line-shape because of the $2f$-modulation.

Only five transions each were recorded in Cologne for $^{13}CH_3CN$ and $CH_3^{13}CN$ at $J'' = 18$ and 16, respectively, and $K = 0-3$ and 6 in order to improve some of the low order spectroscopic parameters. Only in the process of preparing the manuscript was it noted that the residuals between measured frequencies and those calculated from the final set of spectroscopic parameters were considerably smaller than the assumed uncertainties of 3 kHz. In fact, when these transitions were weighted out the average residuals were only 1.9 and 1.5 kHz, respectively. Therefore, uncertainties of 1 kHz were assigned to these transitions. The resulting weighted standard deviations were then 0.303 and 0.571, respectively. This may indicate still too conservative error estimates, but because of the small number of lines which have much smaller uncertainties than most of the transition frequencies such small weighted standard deviations may not mean much.

The present and previous data were fit together to determine spectroscopic parameters for both isotopomers. Higher order parameters which could not be determined reliably were fixed to values derived from the main isotopic species by scaling the parameters with appropriate powers of B and taking into consideration deviations from this estimate for related lower order parameters. The results are also given in Table 2. The newly measured transition frequencies are given in Tables 4 and 5 toward the end of the manuscript together with their assignments, uncertainties, and the residuals between measured frequencies and those calculated from the final spectroscopic parameters.

The rotational and centrifugal distortion parameters have been improved considerably with respect to Pearson & Müller (1996) while the values for eQq are determined entirely from data used in that work. The weighted standard deviations for the whole fits are slightly below 1.0.

3.3. $CH_3C^{15}N$

Pearson & Müller (1996) had in their data set transitions from Bauer et al. (1975) covering 35−143 GHz and from

Demaison et al. (1979) covering 214−232 GHz besides their own measurements. In the present fits we have used the $J = 1-0$ transition frequency from Haekel & Mäder (1989).

The terrestrial $^{14}N/^{15}N$ ratio is about 270, just a factor of three larger than the terrestrial $^{12}C/^{13}C$ ratio. Thus, transitions of this isotopolog were still quite easily observable in samples of natural isotopic composition, see Fig. 1. Eight transitions, $K = 0 - 6$ and 12 for $J'' = 18$ were recorded in Cologne. Additionally, 210 transition frequencies were extracted from the spectra recorded at JPL which extend to $J'' = 66$ near 1.2 THz and to $K = 14$.

The present and previous data were fit together to determine spectroscopic parameters. As in subsection 3.2, higher order parameters were estimated and kept fixed. The spectroscopic parameters are given in Table 2, too. The newly measured transition frequencies are given in Table 6, again toward the end of the manuscript, together with their assignments, uncertainties, and the residuals between measured frequencies and those calculated from the final spectroscopic parameters.

The overall weighted standard deviation is 0.692, and the corresponding values for the transitions recorded in Cologne and at JPL are 0.833 and 0.716.

3.4. CH_2DCN

Le Guennec et al. (1992) presented extensive measurements of the singly deuterated methyl cyanide molecule between 116 and 471 GHz. They were able to observe several of the very weak *b*-type transitions because they employed an isotopically enriched sample. Their data set also included three $J = 2 - 1$ transitions from Thomas et al. (1955).

With transitions of $CH_3C^{15}N$ identified almost as frequently as the singly substituted ^{13}C species it seemed promising to detect CH_2DCN in samples of natural isotopic composition. The terrestrial H/D ratio is about 6400. The presence of three equivalent H atoms decreases the H/D ratio by three, the resolved *K*-doubling for low $K \geq 1$ increases it again by two, and the omission of spin-statistics complicates the situation even more. Altogether, the lines of CH_2DCN are around one order of magnitude weaker than the lines of $CH_3C^{15}N$.

10 lines of 16 transitions with $J'' = 15-18$ and $K \leq 10$ were recorded in Cologne. 109 lines of 152 transitions with $J'' \leq 68$ and $K \leq 11$ were extracted from the spectra taken at JPL. With increasing values of J in the fit it was increasingly difficult to fit the data within experimental uncertainties. It turned out that omission of one of the two very weak $K = 2 \leftrightarrow 1$ transitions reported by Le Guennec et al. (1992) yielded satisfactory fits. Moreover, if one of these transitions was weighted out it appeared as if a 1 MHz typographical error may have occured for the other transition. Since the authors of this work did not have the spectra at their disposal and thus were unable to clarify this issue we decided to omit both $K = 2 \leftrightarrow 1$ transitions from the fit. Without these transitions, D_K could not be determined reliably. Therefore, its value has been estimated by scaling values from ab initio calculations by the ratios of experimental versus ab initio values for CH_3CN (Table 2) and CHD_2CN (Halonen & Mills 1978). The value of 1.97 MHz is slightly bigger than the 1.83 MHz obtained in Le Guennec et al. (1992). H_K was estimated as D_K^2/A as done for CH_3CN, see subsection 3.1. The resulting spectroscopic parameters are given in Table 3. The newly measured transition frequencies are given in Table 7, toward the end of the manuscript, together with their assignments, uncertainties, and the residuals between measured frequencies and those calculated from the final spectroscopic parameters.

Table 3. Spectroscopic parameters[a] (MHz) of monodeuterated methyl cyanide, CH_2DCN and dimensionless weighted standard deviation wrms.

Parameter	Value
A	121 074.677 (20)
B	8 759.197 94 (23)
C	8 608.542 55 (24)
D_K	1.97
$D_{JK} \times 10^3$	143.336 1 (138)
$D_J \times 10^3$	3.469 982 (137)
$d_1 \times 10^6$	−79.164 (46)
$d_2 \times 10^6$	−4.776 (35)
$H_K \times 10^6$	100.
$H_{KJ} \times 10^6$	1.688 (192)
$H_{JK} \times 10^9$	837.5 (49)
$H_J \times 10^{12}$	400.4 (191)
$h_1 \times 10^{12}$	149.0 (84)
$L_{KKJ} \times 10^9$	−10.82 (68)
$L_{JK} \times 10^{12}$	58. (28)
$L_{JJK} \times 10^{12}$	−5.37 (55)
wrms	0.740

[a] Watson's *S* reduction has been used in the representation I^r. Numbers in parentheses are one standard deviation in units of the least significant figures. Parameters without quoted uncertainties have been estimated; see section 3.

The weighted standard deviation for the whole fit is 0.740, for the Cologne and JPL lines it is 0.533 and 0.792, respectively. In particular the uncertainties of the Cologne lines have been estimated somewhat too conservatively.

3.5. $^{13}CH_3^{13}CN$

With even a considerable number of transitions assigned for CH_2DCN it seemed promising to assign transitions of the doubly substituted ^{13}C isotopolog, as the lines are weaker by only about a factor of two. This species should be observable fairly readily in Galactic center sources because of the $^{12}C/^{13}C$ ratio of about 20 in these sources (Wilson & Rood 1994; Müller et al. 2008). Hence, lines of the doubly substituted ^{13}C isotopolog should be only slightly weaker than those of $CH_3C^{15}N$. In fact, inspection of the 3 mm line survey of Sagittarius B2(N) obtained with the IRAM 30 m telecope (A. Belloche, private communication, 2008; see also (Belloche et al. 2009; Müller et al. 2008)) revealed that several $^{13}CH_3^{13}CN$ lines should have S/N ratios of greater than three. However, all lines were overlapped by stronger lines, frequently belonging to the much stronger $^{13}CH_3CN$ which has fairly similar spectroscopic parameters. At higher frequencies, this overlap will be less severe.

Tam et al. (1988) had reported some transition frequencies for this isotopolog up to 72 GHz. Inspection of the broad spectral recordings however failed to produce any even tentative assignments. Subsequently, all spectroscopic parameters were estimated from the isotopologs with no or only one ^{13}C, and only *B* was determined. Still, no assignments could be made.

The search for transitions of $^{13}CH_3^{13}CN$ was the main reason for the measurements in Cologne. Several tentative assignments could be made near 321 GHz. All of these transitions were about 2.8 MHz higher than predicted, suggesting the assumptions of

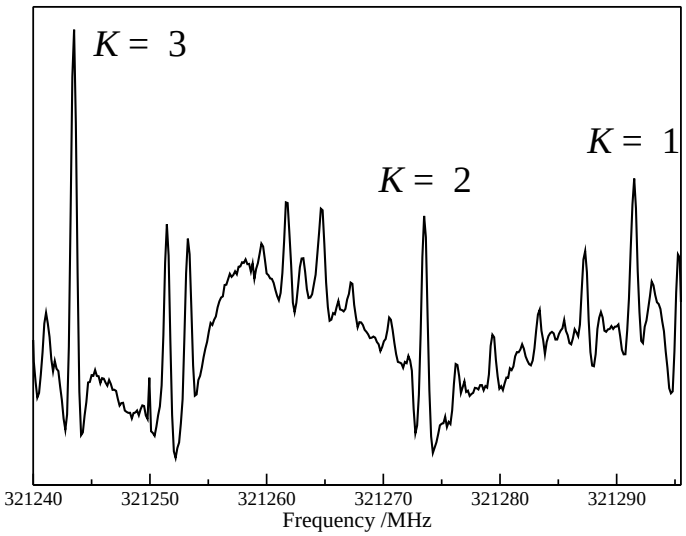

Fig. 2. Section of the lower submillimeter spectrum of CH_3CN. Transitions of $^{13}CH_3^{13}CN$ have been labeled with their K quantum numbers. This isotopolog is less abundant by a factor of 8000 compared to the main isotopolog. While the spectrum is rather sparse on the level of the strongest CH_3CN transitions, it is considerably less sparse on the level of the $CH_3C^{15}N$ transition, see Fig. 1, and rather dense on the level of the $^{13}CH_3^{13}CN$ transitions. One of the lines may be due to a high-K, $v_8 = 1$ line of $^{13}CH_3CN$, all other transitions remain unassigned, see subsection 3.5.

the centrifugal distortion parameters to be good, but the B value to be slightly too small.

With an abundance almost four orders of magnitude smaller than that of the main isotopolog, there are ample chances for overlap. Not only are there many vibrational states of the main isotopolog up to 2000 cm^{-1} which are about as strong or even stronger, but also transitions up to $v_4 = 1$ of the ^{13}C isotopomers, or up to $v_8 = 1$ of the ^{15}N species are about as strong. In addition, many additional species are only slightly weaker, including those of the isotopomers with ^{15}N and one ^{13}C. Even though the rotational spectrum of methyl cyanide is very sparse at the level of the strongest lines of the main isotopolog it is very rich at the level of the $^{13}CH_3^{13}CN$ lines, as can be seen in Fig 2. Only the marked lines belonging to this isotopolog can be assigned unambiguously in this recording. One of the weaker lines may be due to a high-K, $v_8 = 1$ line of $^{13}CH_3CN$, but because of perturbations by $v_8 = 2$, the exact position of this transition is not certain. All other lines can not be assigned at present.

Altogether, 21 transitions with $J'' = 13 - 18$ and $K \leq 6$ were recorded in Cologne. Subsequently, 34 transition with $J'' = 25 - 63$ and $K \leq 9$ could be identified in the spectra taken at JPL. The data from Tam et al. (1988) were omitted from the final fits because their large uncertainties cause negligible effects on the spectroscopic parameters.

Five parameters up to sixth order could be determined with significance; several other were kept fixed to estimated values as done further above (see subsection 3.2). Again, the spectroscopic parameters are listed in Table 2. The measured transition frequencies are given in Table 8, toward the end of the manuscript, together with their assignments, uncertainties, and the residuals between measured frequencies and those calculated from the final spectroscopic parameters.

The weighted standard deviation of the fit is 0.635. It is 0.719 and 0.577 for the data from Cologne and JPL, respectively. The somewhat conservative error estimates can be justified by the possibility that some of the lines may still be affected by overlap to a non-negligible amount. However, the moderately large size of the data set should ensure that such effects are small.

4. Conclusion

Rotational transitions for six astrophysically and astrochemically important isotopologs of methyl cyanide in their ground vibrational states have been recorded and the existing data sets have been extended greatly in most cases. The data should permit reliable predictions to above 2 THz in all instances, sufficient not only for Herschel or ALMA, but very likely also for such missions as SOFIA, CCAT, or others.

Transitions of the even rarer isotopomers containing ^{15}N and one ^{13}C may be observable also, but chance of significant overlap are even higher and the chances to observe these species in space seem vanishingly low.

Predictions of the rotational spectra of the isotopologs studied in the course of the present investigation will be available in the catalog section[1] of the Cologne Database for Molecular Spectroscopy[2] (Müller et al. 2001, 2005). The complete line, parameter and fit files will be deposited in the Spectroscopy Data section of the CDMS. Updated or new JPL catalog (Pickett et al. 1998) entries[3] will be available also.

Acknowledgements. H.S.P.M. is very grateful to the Bundesministerium für Bildung und Forschung (BMBF) for financial support aimed at maintaining the Cologne Database for Molecular Spectroscopy, CDMS. This support has been administered by the Deutsches Zentrum für Luft- und Raumfahrt (DLR). A part of the present research has been carried out at the Jet Propulsion Laboratory, California Institute of Technology, under a contract with the National Aeronautics and Space Administration (NASA).

References

Agúndez, M., Fonfría, J. P., Cernicharo, J., et al. 2008, A&A, 479, 493
Anttila, R., Horneman, V.-M., Koivusaari, M. & Paso, R. 1993, J. Mol. Spectrosc., 157, 198
Bauer, A., Tarrago, G., & Remy, A. 1975, J. Mol. Spectrosc., 58, 111
Belloche, A., Garrod, R. T., Müller, H. S. P., et al. 2009, A&A, 499, 215
Boucher, D., Burie, J., Demaison, J., et al. 1977, J. Mol. Spectrosc., 64, 290
Cazaux, S., Tielens, A. G. G. M., Ceccarelli, C., et al. 2003, ApJ, 593, L51
Cazzoli, G., & Puzzarini, C. 2006, J. Mol. Spectrosc., 240, 153; Erratum, 2008, J. Mol. Spectrosc., 247, 187
Cummins, S. E., Green, S., Thaddeus, P., & Linke, R. A. 1983, ApJ, 266, 331
Demaison, J., Dubrulle, A., Boucher, D., 1979, J. Mol. Spectrosc., 76, 1
Drouin, B. J., Maiwald, F. W., & Pearson, J. C. 2005, Rev. Sci. Instr., 76, Art.-No. 093113
Gadhi, J., Lahrouni, A., Legrand, J., & Demaison, J. 1995, J. Chem. Phys., 92, 1984
Gerin, M., Combes, F., Wlodarczak, et al. 1992, A&A, 259, L35
Haekel, J. & Mäder, H. 1989, J. Quant. Spectrosc. Radiat. Transfer, 41, 9
Halonen, L., & Mills, I. M. 1978, J. Mol. Spectrosc., 73, 494
Kukolich, S. G., Ruben, D. J., Wang, J. H. S., & Williams, J. R. 1973, J. Chem. Phys., 58, 3155
Kukolich, S. G., 1982, J. Chem. Phys., 76, 97
Le Guennec, M., Wlodarczak, G., Burie, J., & Demaison, J. 1992, J. Mol. Spectrosc., 154, 305
Matthews, H. E., & Sears, T. J. 1983, ApJ, 267, L53
Mauersberger, R., Henkel, C., Walmsley, C. M., et al. 1991, A&A, 247, 307
Mito, A., Sakai, J., & Katayama, M. 1984, J. Mol. Spectrosc., 103, 26
Müller, H. S. P., Farhoomand, J., Cohen, E. A., et al. 2000, J. Mol. Spectrosc., 201, 1

[1] website: https://cdms.astro.uni-koeln.de/classic/entries/, see also https://cdms.astro.uni-koeln.de/classic/

[2] website: https://cdms.astro.uni-koeln.de/

[3] website: http://spec.jpl.nasa.gov/ftp/pub/catalog/catdir.html, see also http://spec.jpl.nasa.gov/

Müller, H. S. P., Thorwirth, S., Roth, D. A., & Winnewisser, G. 2001, A&A, 370, L49
Müller, H. S. P., Schlöder, F., Stutzki, J., & Winnewisser, G. 2005, J. Mol. Struct, 742, 215
Müller, H. S. P., & Brünken, S. 2005, J. Mol. Spectrosc., 232, 213
Müller, H. S. P., McCarthy, M. C., Bizzocchi, L., et al. 2007a, Phys. Chem. Chem. Phys., 9, 1579
Müller, H. S. P., Drouin, B. J., Pearson, J. C., et al. 2007b, contribution WG03, presented at the 62nd International Symposium on Molecular Spectroscopy, June 18 22, 2007, Columbus, Ohio, USA; see also http://molspect.chemistry.ohio-state.edu/symposium_62/symposium/Abstracts/p074.pdf
Müller, H. S. P., Belloche, A., Menten, K. M., et. al. 2008, J. Mol. Spectrosc., 251, 319
Nummelin, A., Bergman, P., Hjalmarson, Å., et al. 1998, ApJS, 117, 427
Pavone, F. S., Zink, L. R., Prevedelli, M., et al. 1990, J. Mol. Spectrosc., 144, 45
Pearson, J. C., & Müller, H. S. P. 1996, ApJ, 471, 1067
Pickett, H. M., Poynter, R. L., Cohen, E. A., et al. 1998, J. Quant. Spectrosc. Radiat. Transfer, 60, 883
Ring, H., Edwards, H., Kessler, M., & Gordy, W. 1947, Phys. Rev., 72, 1262
Šimečková, M., Urban, Š., Fuchs, U., et al. 2004, J. Mol. Spectrosc., 226, 123
Solomon, P. M., Jefferts, K. B., Penzias, A. A., & Wilson, R. W. 1971, ApJ, 168, L107
Sutton, E. C., Blake, G. A., Masson, C. R., & Phillips, T. G. 1985, ApJS, 58, 341
Tam, H., An, I., & Roberts, J. A. 1988, J. Mol. Spectrosc., 129, 202
Thomas, L. F., Sherrard, E. J. & Sheridan, J. 1955, Trans. Faraday Soc., 51, 619
Ulich, B. L., & Conklin, E. K. 1974, Nature, 248, 121
Wilson, T. L., & Rood, R. 1994, ARA&A, 32, 191
Winnewisser, G., Krupnov, A. F., Tretyakov, M. Y., et al. 1994, J. Mol. Spectrosc., 165, 294

Table 4. Lower state quantum numbers of rotational transitions of $^{13}CH_3CN$ from present work, frequencies (MHz), uncertainties unc. (kHz), and residuals o−c (kHz) between observed frequencies and those calculated from the final set of spectroscopic parameters.

J''	K''	frequency	unc.	o−c	J''	K''	frequency	unc.	o−c	J''	K''	frequency	unc.	o−c
18	6	339137.3433	1.0	−0.3	43	0	784895.847	50	43	56	3	1015544.407	20	21
18	3	339309.0082	1.0	0.3	44	12	800553.654	150	−143	56	2	1015636.946	30	17
18	2	339340.8330	1.0	0.4	44	11	800891.319	100	−105	56	1	1015692.486	30	17
18	1	339359.9326	1.0	−0.0	44	10	801200.157	50	13	56	0	1015711.009	50	24
18	0	339366.2998	1.0	−0.4	44	9	801479.794	50	−44	57	12	1030736.928	150	51
24	12	445241.735	30	−11	44	8	801730.374	50	−18	57	10	1031558.219	50	63
24	11	445432.247	50	73	44	7	801951.637	50	−72	57	8	1032231.921	30	22
24	10	445606.353	50	51	44	6	802143.651	50	−47	57	7	1032513.150	20	46
24	9	445764.100	50	41	44	5	802306.261	50	−22	57	6	1032757.054	20	10
24	8	445905.405	30	22	44	4	802439.367	50	−30	57	5	1032963.632	20	11
24	7	446030.264	30	48	44	3	802542.979	50	−7	57	4	1033132.760	20	7
24	6	446138.527	20	19	44	2	802616.938	50	−71	57	2	1033358.435	20	14
24	5	446230.222	20	8	44	1	802661.445	50	10	57	1	1033414.879	20	12
24	4	446305.355	50	56	44	0	802676.201	50	−44	57	0	1033433.720	20	35
24	3	446363.747	20	17	45	9	819230.822	100	−149	60	12	1083745.465	50	−34
24	2	446405.494	20	11	45	8	819486.798	100	−45	60	11	1084195.000	50	−0
24	1	446430.566	20	24	45	7	819712.787	50	−70	60	9	1084978.318	50	−54
24	0	446438.899	20	3	45	6	819908.940	50	20	60	8	1085311.933	50	−4
25	12	463032.948	50	70	45	5	820075.010	50	54	60	6	1085862.162	50	−1
25	11	463230.857	50	42	45	4	820210.775	50	−120	60	4	1086255.771	50	−44
25	10	463411.809	80	2	45	3	820316.536	50	−147	60	3	1086393.678	50	−40
25	9	463575.821	50	38	45	2	820392.237	50	−39	60	2	1086492.216	50	−45
25	6	463965.038	50	45	45	1	820437.489	50	−156	61	13	1100909.779	100	92
25	5	464060.345	50	31	45	0	820452.748	50	−22	61	12	1101404.872	50	11
25	4	464138.400	50	41	46	9	836978.116	50	−59	61	10	1102278.334	80	−15
25	3	464199.111	50	18	46	8	837239.242	80	−108	61	9	1102656.306	30	−19
25	2	464242.534	50	42	46	7	837469.939	50	−107	61	7	1103293.992	20	−5
25	1	464268.543	50	3	46	6	837670.126	50	−46	61	6	1103553.424	20	−17
25	0	464277.228	50	5	46	5	837839.510	50	−137	61	5	1103773.128	50	−18
26	13	480598.910	200	15	46	4	837978.301	50	−102	61	4	1103953.032	20	5
26	12	480821.850	100	20	46	3	838086.283	50	−99	61	3	1104093.012	20	4
26	10	481215.078	50	−26	46	2	838163.526	50	−15	61	2	1104193.040	20	4
26	9	481385.284	50	−5	46	1	838209.741	50	−109	61	1	1104253.061	20	−8
26	8	481537.813	50	67	46	0	838225.208	50	−81	61	0	1104273.082	20	−0
26	7	481672.435	50	22	49	12	889171.685	80	46	62	13	1118556.496	100	4
26	6	481789.313	50	78	49	11	889544.894	100	15	62	12	1119059.047	50	54
26	5	481888.243	100	77	49	10	889886.195	80	32	62	11	1119522.099	80	76
26	4	481969.220	50	55	49	9	890195.361	80	5	62	10	1119945.421	40	16
26	3	482032.241	50	42	49	8	890472.317	50	−20	62	8	1120672.581	20	6
26	2	482077.319	50	78	49	7	890716.982	50	−12	62	7	1120976.075	20	−1
26	1	482104.227	50	−48	49	6	890929.260	50	28	62	6	1121239.357	50	−1
26	0	482113.311	50	24	49	5	891108.967	50	4	62	5	1121462.318	20	5
27	12	498608.539	150	24	49	4	891256.131	50	16	62	3	1121786.918	20	12
27	11	498821.247	150	−178	49	3	891370.650	50	21	62	2	1121888.415	20	1
27	10	499016.263	100	151	49	2	891452.462	50	5	62	1	1121949.341	20	7
27	8	499350.520	50	18	49	1	891501.579	50	12	62	0	1121969.656	30	12
27	7	499490.120	50	47	49	0	891517.973	50	33	63	15	1135059.113	150	40
27	6	499611.153	50	4	50	13	906470.254	150	42	63	11	1137177.559	50	−3
27	5	499713.686	50	4	50	12	906882.928	50	9	63	10	1137607.095	30	4
27	4	499797.648	50	17	50	11	907263.229	80	15	63	9	1137996.224	20	−3
27	2	499909.654	50	11	50	10	907610.895	100	−53	63	8	1138344.827	50	9
27	1	499937.687	50	27	50	9	907925.987	50	1	63	7	1138652.740	20	15
27	0	499947.025	50	24	50	8	908208.205	50	3	63	6	1138919.837	20	8
28	11	516613.238	80	10	50	7	908457.487	80	4	63	5	1139146.023	20	2
28	10	516814.764	80	23	50	6	908673.729	50	−2	63	4	1139331.185	50	−27
28	9	516997.294	50	−16	50	5	908856.837	50	−22	63	3	1139475.324	20	−2
28	3	517691.313	50	22	50	4	909006.769	50	−23	63	2	1139578.300	20	−7
28	2	517739.642	50	31	50	3	909123.446	50	−23	63	1	1139640.092	20	−19
28	1	517768.629	50	19	50	2	909206.838	50	−7	64	14	1153276.801	200	131
28	0	517778.310	50	31	50	1	909256.926	50	43	64	12	1154351.199	30	−21
34	16	621760.772	50	10	50	0	909273.539	50	−26	64	9	1155657.985	20	−18
34	14	622447.422	30	−26	51	12	924589.926	80	22	64	8	1156011.566	20	4
34	11	623309.671	20	14	51	11	924977.218	100	−13	64	7	1156323.830	20	−27
34	10	623551.857	20	5	51	9	925652.265	50	8	64	6	1156594.758	20	−9

Table 4. continued.

J''	K''	frequency	unc.	o−c	J''	K''	frequency	unc.	o−c	J''	K''	frequency	unc.	o−c
34	9	623771.262	20	−14	51	8	925939.684	50	−7	64	4	1157012.016	20	5
34	7	624141.443	20	−28	51	7	926193.576	80	−5	64	3	1157158.166	20	−13
34	6	624292.087	20	−5	51	5	926600.341	80	2	64	2	1157262.634	20	8
34	4	624524.053	20	−26	51	4	926753.052	80	8	64	0	1157346.208	20	−2
34	2	624663.446	20	24	51	3	926871.878	50	−0	65	13	1171464.851	100	10
34	1	624698.263	20	−13	51	2	926956.781	50	−14	65	11	1172472.160	80	−102
34	0	624709.879	20	−16	51	1	927007.756	50	−2	65	9	1173314.209	30	−5
35	16	639490.666	100	54	51	0	927024.756	50	8	65	8	1173672.712	20	−8
35	14	640196.404	60	27	55	12	995373.248	100	44	65	6	1174264.072	20	−12
35	12	640810.267	30	−44	55	10	996168.138	100	60	65	4	1174687.142	50	−23
35	11	641082.493	50	−47	55	9	996511.966	50	−72	65	3	1174835.374	20	−3
35	9	641556.961	50	−22	55	7	997092.349	20	21	65	2	1174941.285	20	−1
35	7	641937.464	20	1	55	5	997528.396	20	33	65	1	1175004.858	20	9
35	6	642092.248	50	−20	55	4	997692.055	20	−4	65	0	1175026.016	30	−23
35	5	642223.312	50	−53	55	3	997819.444	30	−3	66	12	1189621.606	120	111
35	4	642330.670	30	−28	55	2	997910.473	20	−2	66	11	1190111.236	150	−17
35	3	642414.174	50	−52	55	1	997965.147	30	40	66	10	1190558.963	120	−107
35	2	642473.884	30	−29	55	0	997983.325	20	6	66	9	1190964.780	20	6
35	0	642521.653	30	−24	56	12	1013057.279	100	−164	66	6	1191927.684	25	−10
43	8	783970.101	80	18	56	9	1014215.234	20	7	66	5	1192163.522	20	8
43	6	784374.602	50	11	56	8	1014528.429	50	−48	66	4	1192356.610	20	23
43	5	784533.705	50	−10	56	7	1014805.211	20	40	66	3	1192506.829	20	−6
43	3	784765.344	50	−36	56	6	1015045.237	30	40	66	2	1192614.182	20	−17
43	2	784837.839	50	11	56	5	1015248.484	20	23	66	1	1192678.616	20	−19
43	1	784881.204	50	−104	56	4	1015414.879	20	−1	66	0	1192700.114	20	−2

Table 5. Lower state quantum numbers of rotational transitions of $CH_3^{13}CN$ from present work, frequencies (MHz), uncertainties unc. (kHz), and residuals o−c (kHz) between observed frequencies and those calculated from the final set of spectroscopic parameters.

J''	K''	frequency	unc.	o−c	J''	K''	frequency	unc.	o−c	J''	K''	frequency	unc.	o−c
16	6	312317.7600	1.0	0.1	34	1	642938.809	50	−45	53	3	990423.344	50	−29
16	3	312479.1625	1.0	0.2	34	0	642950.994	50	−54	53	2	990515.635	20	−1
16	2	312509.0842	1.0	0.1	41	6	770673.135	50	−47	53	1	990571.014	20	6
16	1	312527.0409	1.0	−1.1	41	4	770963.549	50	−25	53	0	990589.492	20	24
16	0	312533.0294	1.0	0.6	41	3	771065.296	50	−8	54	6	1008167.091	30	44
23	10	440278.491	50	−21	41	2	771137.916	50	−81	54	4	1008542.013	30	25
23	9	440437.626	20	20	41	1	771181.580	50	−45	54	2	1008767.251	50	58
23	8	440580.110	20	−13	41	0	771196.159	50	−11	54	1	1008823.503	30	−19
23	7	440706.004	20	−5	42	10	788019.367	150	−162	54	0	1008842.357	50	57
23	6	440815.253	20	40	42	9	788300.498	50	10	55	9	1025547.406	30	34
23	5	440907.717	20	25	42	8	788552.113	50	−61	55	8	1025870.459	50	−6
23	4	440983.429	30	22	42	7	788774.377	50	−108	55	7	1026155.838	50	−13
23	1	441109.693	20	−8	42	6	788967.211	50	−125	55	6	1026403.441	50	25
23	0	441118.148	20	23	42	5	789130.563	50	−86	55	4	1026784.724	30	22
24	12	458222.531	120	20	42	4	789264.223	80	−135	55	3	1026918.341	50	68
24	11	458422.402	120	−48	42	3	789368.387	50	−24	55	2	1027013.731	20	11
24	10	458605.156	120	−114	42	2	789442.628	80	−135	55	1	1027071.016	20	14
24	7	459050.448	50	118	42	1	789487.346	50	−40	55	0	1027090.097	20	−2
24	6	459164.066	50	45	42	0	789502.201	50	−62	56	12	1042550.491	50	34
24	5	459260.263	50	−36	43	12	805624.829	80	−124	56	11	1042993.029	50	−55
24	4	459339.106	50	−18	43	10	806288.633	50	−59	56	10	1043397.819	30	14
24	3	459400.506	50	40	43	9	806575.857	50	−47	56	9	1043764.461	30	−1
24	2	459444.289	50	−10	43	8	806833.106	50	−84	56	8	1044092.961	20	46
24	1	459470.550	50	−57	43	7	807060.397	50	−53	56	7	1044383.048	30	15
24	0	459479.378	50	1	43	6	807257.542	50	−50	56	4	1045022.335	30	24
25	12	476531.946	80	−16	43	5	807424.442	100	−97	56	2	1045255.204	30	79
25	10	476929.757	80	−44	43	4	807561.186	50	−37	56	1	1045313.390	20	32
25	9	477101.989	50	35	43	3	807667.545	50	−46	56	0	1045332.804	20	33
25	8	477256.174	50	1	43	2	807743.522	50	−77	60	13	1114776.860	50	−32
25	7	477392.405	50	11	43	1	807789.195	50	−20	60	12	1115288.291	20	−4
25	6	477510.574	50	11	43	0	807804.377	50	−46	60	10	1116190.390	20	−1
25	5	477610.680	50	46	44	7	825342.348	100	−89	60	9	1116580.728	20	−11

Table 5. continued.

J''	K''	frequency	unc.	o−c	J''	K''	frequency	unc.	o−c	J''	K''	frequency	unc.	o−c
25	4	477692.603	50	39	44	6	825543.773	50	−85	60	8	1116930.416	20	6
25	3	477756.356	50	33	44	5	825714.366	100	−62	60	7	1117239.270	20	−0
25	2	477801.869	50	−14	44	4	825853.985	50	−94	60	6	1117507.196	20	−2
25	1	477829.257	50	30	44	2	826040.390	50	−22	60	5	1117734.082	50	−4
25	0	477838.379	50	37	44	1	826086.880	50	−138	60	4	1117919.833	20	−13
26	12	494839.226	50	102	45	12	842122.594	150	−45	60	2	1118167.698	20	−0
26	11	495054.907	100	104	45	10	842814.997	120	−150	60	1	1118229.675	20	−17
26	10	495252.014	50	−0	45	9	843114.715	80	−93	60	0	1118250.348	20	−12
26	9	495430.686	50	4	47	13	878195.374	150	79	61	9	1134771.355	50	23
26	8	495590.783	50	47	47	12	878604.078	80	−4	61	8	1135126.272	20	17
26	7	495732.066	50	−44	47	11	878980.835	80	76	61	7	1135439.732	30	−20
26	6	495854.766	50	16	47	10	879325.220	50	39	61	6	1135711.703	20	−1
26	4	496043.684	50	47	47	9	879637.230	50	18	61	5	1135941.998	20	−1
26	3	496109.798	50	−9	47	8	879916.758	50	27	61	2	1136382.127	20	6
26	2	496157.109	50	18	47	7	880163.650	50	22	61	1	1136445.038	30	−8
26	1	496185.478	50	8	47	6	880377.805	50	0	61	0	1136466.018	20	−6
26	0	496194.930	50	0	47	5	880559.094	100	−84	62	15	1149921.646	50	6
27	12	513143.945	80	36	47	4	880707.708	50	35	62	14	1150530.560	50	37
27	10	513571.914	100	91	47	3	880823.252	100	21	62	12	1151625.207	50	36
27	9	513757.039	50	47	47	2	880905.815	50	10	62	11	1152110.498	30	−25
27	8	513922.895	50	26	47	1	880955.373	50	10	62	10	1152554.304	30	−3
27	7	514069.366	50	−21	47	0	880971.914	50	29	62	8	1153316.508	20	3
27	6	514196.520	50	29	48	13	896421.629	120	−9	62	7	1153634.632	25	10
27	5	514304.162	50	36	48	12	896838.549	80	59	62	6	1153910.575	20	−3
27	4	514392.277	50	27	48	10	897573.823	80	10	62	5	1154144.275	20	9
27	3	514460.821	50	−8	48	9	897892.002	50	2	62	4	1154335.590	20	−2
27	2	514509.842	50	9	48	8	898177.045	50	13	62	2	1154590.861	20	−11
27	1	514539.243	50	−0	48	7	898428.827	50	27	62	1	1154654.718	20	−5
27	0	514549.047	50	−1	48	6	898647.220	50	19	62	0	1154676.018	20	8
33	15	621969.166	30	40	48	4	898983.584	50	9	63	12	1169785.281	20	−4
33	14	622308.158	30	−16	48	2	899185.623	50	8	63	11	1170277.655	30	0
33	13	622624.402	20	−16	48	1	899236.139	50	−12	63	10	1170727.840	30	−15
33	10	623435.148	30	−11	48	0	899253.011	50	13	63	9	1171135.718	40	5
33	9	623659.045	20	−13	49	13	914643.473	200	−207	63	7	1171823.773	20	−14
33	8	623859.664	20	34	49	10	915818.023	150	−47	63	6	1172103.723	20	−9
33	7	624036.764	20	−31	49	9	916142.366	50	−25	63	5	1172340.795	25	−2
33	6	624190.451	20	−31	49	8	916432.928	50	8	63	4	1172534.868	40	−21
33	5	624320.650	20	21	49	7	916689.536	50	−4	63	2	1172793.840	25	−19
33	4	624427.221	30	36	49	6	916912.168	50	16	63	1	1172858.675	40	42
33	3	624510.071	30	−36	49	4	917255.016	50	5	63	0	1172880.216	20	−11
33	2	624569.356	20	−5	49	2	917460.920	50	−26	64	12	1187939.602	120	−128
33	0	624616.735	30	−42	49	1	917512.445	50	−10	64	11	1188438.974	150	−112
34	15	640227.661	40	8	49	0	917529.610	50	−17	64	10	1188895.674	30	−1
34	14	640576.289	60	−112	53	13	987487.235	200	170	64	9	1189309.325	20	4
34	13	640901.691	30	−2	53	11	988364.813	80	104	64	8	1189679.851	25	−11
34	11	641481.367	50	−52	53	10	988749.584	50	37	64	7	1190007.145	30	−12
34	8	642172.196	30	−45	53	9	989098.196	20	3	64	6	1190291.073	20	−1
34	7	642354.446	30	−28	53	8	989410.512	20	1	64	5	1190531.497	20	−5
34	4	642756.021	20	−12	53	7	989686.393	20	15	64	4	1190728.334	30	−13
34	3	642841.300	20	−26	53	6	989925.693	20	7	64	2	1190990.978	20	−13
34	2	642902.247	30	−28	53	4	990294.279	20	22	64	1	1191056.621	50	−63

Table 6. Lower state quantum numbers of rotational transitions of $CH_3C^{15}N$ from present work, frequencies (MHz), uncertainties unc. (kHz), and residuals o−c (kHz) between observed frequencies and those calculated from the final set of spectroscopic parameters.

J''	K''	frequency	unc.	o−c	J''	K''	frequency	unc.	o−c	J''	K''	frequency	unc.	o−c
18	12	338023.606	10	0	35	11	640278.287	70	−75	56	7	1013569.196	30	51
18	6	338710.019	8	−8	35	9	640754.725	30	−9	56	6	1013809.982	30	−23
18	5	338780.216	3	1	35	7	641136.691	50	−38	56	5	1014014.014	50	45
18	4	338837.680	3	1	35	6	641292.126	40	−18	56	4	1014180.965	20	7
18	3	338882.394	3	−4	35	4	641531.486	30	−18	56	3	1014310.943	50	36
18	2	338914.344	8	−8	35	3	641615.332	50	−23	56	2	1014403.766	20	3

Table 6. continued.

J''	K''	frequency	unc.	o−c	J''	K''	frequency	unc.	o−c	J''	K''	frequency	unc.	o−c
18	1	338933.536	5	6	35	2	641675.251	20	−22	56	1	1014459.492	30	−0
18	0	338939.926	5	2	35	1	641711.248	20	16	56	0	1014478.090	50	19
24	12	444677.654	50	68	44	12	799556.798	100	−10	57	8	1030975.149	50	27
24	11	444868.773	80	−60	44	11	799895.712	80	−58	57	6	1031502.077	20	−9
24	10	445043.705	50	5	44	9	800486.471	50	−2	57	5	1031709.364	30	−6
24	9	445202.122	50	2	44	8	800737.904	100	−84	57	4	1031879.082	20	6
24	7	445469.416	50	36	44	7	800960.070	50	−74	57	3	1032011.155	20	15
24	6	445578.097	50	−19	44	6	801152.797	50	−59	57	2	1032105.530	20	23
24	5	445670.197	50	1	44	5	801315.982	50	−66	57	1	1032162.147	20	4
24	4	445745.587	50	4	44	4	801449.656	50	−1	57	0	1032181.021	20	−4
24	3	445804.286	50	36	44	3	801553.593	50	−37	60	8	1083996.412	30	−21
24	2	445846.202	50	31	44	2	801627.891	50	−35	60	7	1084292.050	50	−17
24	1	445871.360	50	29	44	1	801672.512	50	−2	60	5	1084765.613	80	−70
24	0	445879.744	50	26	44	0	801687.390	50	10	60	3	1085081.878	50	41
25	11	462645.335	100	10	45	5	819063.889	50	−13	60	1	1085240.023	20	−15
25	10	462827.117	100	34	45	4	819200.272	50	−71	60	0	1085259.811	20	−9
25	9	462991.739	50	−7	45	3	819306.491	50	−29	61	10	1100941.061	50	29
25	8	463139.273	50	22	45	2	819382.243	80	−148	61	9	1101320.232	50	−73
25	7	463269.567	50	28	46	9	835943.102	150	−54	61	6	1102220.449	20	8
25	6	463382.606	50	46	46	6	836637.725	80	−26	61	5	1102440.856	30	−18
25	5	463478.295	50	26	46	5	836807.842	80	−10	61	3	1102761.793	20	8
25	4	463556.690	50	63	46	4	836947.184	80	67	61	2	1102862.131	20	−7
25	3	463617.624	50	18	46	3	837055.463	50	−29	61	0	1102942.430	20	−14
25	2	463661.238	50	58	46	2	837132.851	50	−82	62	12	1117699.499	200	171
25	1	463687.317	50	−13	46	1	837179.357	50	−52	62	10	1118588.819	30	3
25	0	463696.065	50	17	49	12	888070.867	100	3	62	9	1118973.704	30	16
26	12	480213.412	100	51	49	11	888445.580	120	42	62	8	1119318.436	20	−11
26	11	480419.811	100	143	49	10	888788.116	100	−1	62	7	1119622.944	20	−18
26	9	480779.185	50	−16	49	9	889098.523	50	52	62	6	1119887.123	20	11
26	8	480932.181	80	−107	49	6	889835.075	50	23	62	5	1120110.797	20	−2
26	7	481067.510	50	2	49	5	890015.474	50	40	62	4	1120293.942	20	8
26	6	481184.797	50	−9	49	4	890163.134	50	17	62	3	1120436.478	30	32
26	5	481284.187	50	49	49	3	890278.046	50	5	63	11	1135800.408	120	63
26	4	481365.532	50	70	49	2	890360.170	50	7	63	8	1136971.561	30	17
26	3	481428.740	50	−8	49	1	890409.470	50	21	63	6	1137548.452	20	5
26	2	481473.947	50	−23	49	0	890425.897	50	18	63	5	1137775.379	20	6
26	1	481501.168	50	56	50	11	906143.305	150	−87	63	4	1137961.166	20	5
26	0	481510.165	50	6	50	10	906492.536	80	97	63	3	1138105.724	20	−14
27	9	498564.375	50	−25	50	9	906808.668	50	17	63	2	1138209.052	20	5
27	8	498723.057	100	−3	50	8	907091.879	80	−30	63	1	1138271.082	30	32
27	7	498863.213	80	12	50	7	907342.068	80	−35	64	11	1153431.417	80	18
27	6	498984.839	50	69	50	6	907559.150	50	15	64	10	1153868.550	50	26
27	5	499087.724	50	8	50	5	907742.947	50	25	64	8	1154619.250	30	−3
27	3	499237.616	50	24	50	4	907893.365	50	−27	64	7	1154932.519	80	−51
27	2	499284.459	50	−1	50	3	908010.479	50	−7	64	6	1155204.355	30	−4
27	0	499322.004	50	38	51	12	923448.206	100	−16	64	5	1155434.482	30	−29
28	9	516347.309	80	49	51	10	924192.510	100	−0	64	4	1155622.929	20	−12
28	8	516511.508	50	27	51	9	924514.553	80	−9	64	3	1155769.523	80	−50
28	7	516656.554	50	18	51	8	924803.059	50	10	64	2	1155874.320	80	−32
28	6	516782.448	50	82	51	7	925057.871	50	9	64	1	1155937.201	30	−34
28	5	516888.896	50	−26	51	6	925278.880	50	−21	64	0	1155958.150	30	−49
28	3	517044.107	50	56	51	5	925466.075	50	−6	65	9	1171901.821	30	10
34	13	621972.452	50	−23	51	4	925619.334	50	5	65	8	1172261.466	30	−24
34	12	622261.132	50	8	51	3	925738.595	50	11	65	7	1172579.205	30	23
34	11	622527.126	30	33	51	2	925823.803	50	3	65	5	1173088.143	20	15
34	9	622990.550	50	−45	51	1	925874.943	50	0	65	3	1173427.860	50	−7
34	8	623187.975	20	24	51	0	925891.997	50	4	65	2	1173534.097	20	−11
34	6	623513.510	20	21	55	10	994948.576	150	−48	65	0	1173619.153	20	28
34	5	623641.561	20	17	55	8	995602.961	80	−85	66	12	1188185.703	150	−111
34	4	623746.418	40	34	55	7	995876.199	50	26	66	9	1189533.633	80	73
34	3	623827.915	50	−56	55	6	996113.103	50	6	66	7	1190220.192	30	−24
34	2	623886.265	20	−4	55	5	996313.763	50	33	66	6	1190499.574	30	−01
34	1	623921.231	30	−27	55	3	996605.769	50	−48	66	5	1190736.074	100	−64
34	0	623932.881	30	−41	55	2	996697.183	50	27	66	4	1190929.820	50	4
35	14	639388.490	150	4	55	1	996752.051	50	77	66	2	1191188.194	50	−36
35	13	639708.307	100	−38	55	0	996770.268	50	19	66	1	1191252.892	30	27
35	12	640004.964	40	−44	56	9	1012977.101	30	−21					

Table 7. Quantum numbers of rotational transitions of CH_2DCN from present work, frequencies (MHz), uncertainties unc. (kHz), and residuals o−c (kHz) between observed frequencies and those calculated from the final set of spectroscopic parameters.

$J', K'_a, K'_c - J'', K''_a, K''^a_c$	frequency	unc.	o−c	$J', K'_a, K'_c - J'', K''_a, K''^a_c$	frequency	unc.	o−c
16, 5, d − 15, 5, d	277717.406	15	1	52, 2, 50 − 51, 2, 49	903537.321	100	79
16, 4, d − 15, 4, d	277761.128	8	0	52, 1, 51 − 51, 1, 50	904004.487	200	−106
16, 1, 15 − 15, 1, 14	279000.540	8	−4	53, 1, 53 − 52, 1, 52	913688.193	200	−117
18, 10, d − 17, 10, d	312026.460	30	−33	53, 5, d − 52, 5, d	918213.532	200	244
18, 9, d − 17, 9, d	312124.485	25	−1	53, 2, 51 − 52, 2, 50	920897.991	200	−104
18, 8, d − 17, 8, d	312212.301	20	−22	53, 1, 52 − 52, 1, 51	921264.278	200	−12
19, 1, 19 − 18, 1, 18	328415.596	20	−4	57, 0, 57 − 56, 0, 56	983638.923	200	221
19, 10, d − 18, 10, d	329351.951	30	−5	57, 7, d − 56, 7, d	986718.597	200	−83
19, 3, 17 − 18, 3, 16	329864.188	20	−3	57, 6, d − 56, 6, d	986958.857	100	25
19, 2, 17 − 18, 2, 16	330013.795	10	2	57, 5, d − 56, 5, d	987192.298	100	−104
28, 2, 26 − 27, 2, 25	486412.193	50	−14	57, 3, 54 − 56, 3, 53	988062.351	150	64
28, 6, d − 27, 6, d	485722.367	50	55	57, 1, 56 − 56, 1, 55	990226.073	150	−131
28, 5, d − 27, 5, d	485817.005	50	17	59, 0, 59 − 58, 0, 58	1017787.045	100	−42
28, 2, 27 − 27, 2, 26	485869.754	50	29	59, 3, 56 − 58, 3, 55	1022618.283	200	305
28, 4, d − 27, 4, d	485902.358	50	2	59, 2, 57 − 58, 2, 56	1024977.054	200	138
28, 3, 26 − 27, 3, 25	485983.562	50	−53	60, 1, 60 − 59, 1, 59	1033530.934	200	−76
28, 3, 25 − 27, 3, 24	485997.103	50	86	60, 2, 59 − 59, 2, 58	1038125.138	200	458
28, 8, d − 27, 8, d	485492.763	50	21	60, 1, 59 − 59, 1, 58	1041862.576	200	330
28, 7, d − 27, 7, d	485614.775	50	69	60, 2, 58 − 59, 2, 57	1042306.148	250	−269
28, 10, d − 27, 10, d	485203.300	120	−60	63, 1, 63 − 62, 1, 62	1084807.020	150	−95
28, 9, d − 27, 9, d	485355.715	120	−32	63, 0, 63 − 62, 0, 62	1086011.334	100	−55
28, 1, 27 − 27, 1, 26	487942.201	80	8	63, 10, d − 62, 10, d	1089039.445	200	160
29, 4, d − 28, 4, d	503235.929	50	4	63, 9, d − 62, 9, d	1089381.592	150	−123
29, 3, 27 − 28, 3, 26	503321.438	100	−2	63, 2, 62 − 62, 2, 61	1089618.582	80	11
29, 3, 26 − 28, 3, 25	503337.368	100	−40	63, 8, d − 62, 8, d	1089695.853	200	177
29, 2, 27 − 28, 2, 26	503793.683	50	−15	63, 7, d − 62, 7, d	1089985.064	80	29
30, 8, d − 29, 8, d	520124.625	80	0	63, 6, d − 62, 6, d	1090257.213	80	−35
30, 6, d − 29, 6, d	520371.360	100	−16	63, 5, d − 62, 5, d	1090528.555	100	1
30, 3, 28 − 29, 3, 27	520657.371	100	155	63, 4, 60 − 62, 4, 59	1090822.850	80	−22
30, 3, 27 − 29, 3, 26	520676.142	100	14	63, 4, 59 − 62, 4, 58	1090859.365	120	−65
30, 2, 28 − 29, 2, 27	521175.868	100	−24	63, 3, 60 − 62, 3, 59	1091699.685	80	31
31, 1, 31 − 30, 1, 30	535476.485	100	21	63, 1, 62 − 62, 1, 61	1093420.205	80	13
36, 1, 36 − 35, 1, 35	621614.941	30	−32	64, 10, d − 63, 10, d	1106217.421	200	−65
36, 11, d − 35, 11, d	623372.367	100	24	64, 7, d − 63, 7, d	1107179.127	80	44
36, 0, 36 − 35, 0, 35	623466.170	70	−63	64, 1, 63 − 63, 1, 62	1110587.991	120	−91
36, 10, d − 35, 10, d	623587.841	50	−40	64, 2, 62 − 63, 2, 61	1111566.310	200	175
36, 9, d − 35, 9, d	623783.719	100	−30	65, 1, 65 − 64, 1, 64	1118961.766	200	224
36, 7, d − 35, 7, d	624118.615	50	30	65, 0, 65 − 64, 0, 64	1120088.060	200	−151
36, 6, d − 35, 6, d	624259.658	70	−55	65, 8, d − 64, 8, d	1124068.425	200	150
36, 2, 35 − 35, 2, 34	624357.951	50	81	65, 6, d − 64, 6, d	1124651.425	200	25
36, 5, d − 35, 5, d	624386.762	70	−54	65, 4, 62 − 64, 4, 61	1125246.197	150	32
36, 3, 33 − 35, 3, 32	624671.021	50	56	65, 3, 62 − 64, 3, 61	1126225.423	200	210
36, 2, 34 − 35, 2, 33	625480.300	40	−32	65, 1, 64 − 64, 1, 63	1127746.725	100	50
37, 1, 37 − 36, 1, 36	638831.212	30	−51	65, 2, 63 − 64, 2, 62	1128865.300	120	71
37, 11, d − 36, 11, d	640652.376	100	−27	66, 4, 63 − 65, 4, 62	1142450.318	100	−121
37, 10, d − 36, 10, d	640873.836	70	−23	66, 4, 62 − 65, 4, 61	1142500.850	100	70
37, 9, d − 36, 9, d	641075.115	50	−46	66, 3, 64 − 65, 3, 63	1142588.221	120	13
37, 8, d − 36, 8, d	641256.800	50	4	66, 1, 65 − 65, 1, 64	1144895.808	200	−15
37, 5, d − 36, 5, d	641696.453	20	3	66, 2, 64 − 65, 2, 63	1146157.487	50	−17
37, 3, 34 − 36, 3, 33	641996.762	50	−64	67, 1, 67 − 66, 1, 66	1153091.574	200	−94
37, 1, 36 − 36, 1, 35	644319.793	40	−22	67, 10, d − 66, 10, d	1157721.118	200	25
51, 1, 51 − 50, 1, 50	879398.852	150	−74	67, 7, d − 66, 7, d	1158730.616	200	138
51, 6, d − 50, 6, d	883499.518	100	−149	68, 1, 68 − 67, 1, 67	1170147.296	150	−169
51, 5, d − 50, 5, d	883699.093	100	25	68, 0, 68 − 67, 0, 67	1171160.249	80	98
51, 3, 49 − 50, 3, 48	884076.317	150	−113	68, 8, d − 67, 8, d	1175587.939	200	−178
51, 2, 49 − 50, 2, 48	886173.147	200	119	68, 6, d − 67, 6, d	1176204.005	200	−226
52, 1, 52 − 51, 1, 51	896546.406	150	179	68, 1, 67 − 67, 1, 66	1179165.037	200	−191
52, 0, 52 − 51, 0, 51	898157.427	150	45	69, 1, 69 − 68, 1, 68	1187196.902	200	−100
52, 2, 51 − 51, 2, 50	900538.159[b]	150	−1	69, 0, 69 − 68, 0, 68	1188172.743	200	74
52, 7, d − 51, 7, d	900538.159[b]	150	−1	69, 1, 68 − 68, 1, 67	1196285.083	200	−134

[a] A "d" given for K_c signals that the asymmetry doubling has not been resolved for the respective K_a. The uncertainty and the residual refer to the average. Since $J - K_a - K_c = 0$ or 1, K_c is redundant in such case.
[b] Blended lines treated as intensity weighted average in the fit.

Table 8. Lower state quantum numbers of rotational transitions of $^{13}CH_3^{13}CN$, frequencies (MHz), uncertainties unc. (kHz), and residuals o−c (kHz) between observed frequencies and those calculated from the final set of spectroscopic parameters.

J''	K''	frequency	unc.	o−c	J''	K''	frequency	unc.	o−c	J''	K''	frequency	unc.	o−c
13	4	249849.289	30	30	18	5	338978.878	50	2	51	2	926328.788	200	−108
13	3	249881.971	10	−5	18	2	339111.819	15	−6	51	1	926379.428	200	−194
14	4	267689.340	20	−8	25	3	463885.870	50	22	54	3	979425.780	150	20
14	3	267724.401	10	9	25	2	463929.028	50	−11	60	6	1085127.880	150	34
14	2	267749.425	10	−7	27	3	499525.679	100	88	60	4	1085519.654	150	−68
14	1	267764.473	15	12	34	7	623721.761	200	−22	60	3	1085656.847	200	−150
15	6	285421.490	40	21	34	5	623998.639	150	−25	60	0	1085833.407	200	−177
15	4	285528.155	30	18	34	4	624102.519	150	−85	61	9	1101913.821	100	−11
15	3	285565.500	15	−4	34	3	624183.422	100	−68	61	5	1103025.791	150	69
15	2	285592.188	15	−17	34	2	624241.332	50	45	61	4	1103204.664	150	−125
15	1	285608.237	30	7	35	9	641127.171	200	161	61	2	1103443.760	150	55
16	6	303252.220	25	−24	35	3	641980.261	80	−29	61	1	1103503.550	150	88
16	1	303450.598	15	−8	35	1	642075.314	80	−31	62	6	1120480.948	200	154
17	6	321081.547	15	−6	50	3	908507.997	150	−88	62	4	1120884.433	200	−34
17	5	321147.495	20	9	50	2	908591.195	150	123	62	3	1121025.872	100	−3
17	4	321201.474	15	8	50	0	908657.612	150	132	62	2	1121126.880	150	−39
17	3	321243.472	5	−0	51	6	925788.347	200	−80	63	2	1138804.705	200	60
17	2	321273.504	10	15	51	3	926244.313	200	−61	63	1	1138866.331	200	163
17	1	321291.490	15	−13										